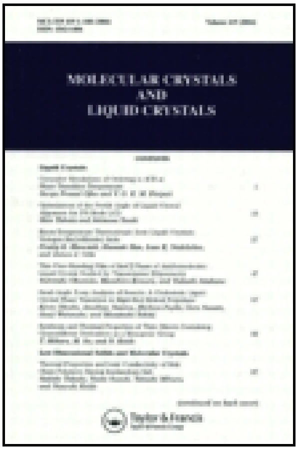

Molecular Crystals and Liquid Crystals Science and Technology. Section A. Molecular Crystals and Liquid Crystals

Publication details, including instructions for authors and subscription information:
http://www.tandfonline.com/loi/gmcl19

Studies of Holographic Gratings Formed in Polymer-Dispersed Liquid Crystal Films and Their Dynamical Behavior

Andy Ying-Guey Fuh [a], Tsung-Chin Ko [a], Ming-Shann Tsai [a], Chi-Yen Huang [a] & Liang-Chy Chien [a b]

[a] Department of Physics, National Cheng-Kung University, Tainan, Taiwan, 701, ROC

[b] Chemical physics, ALCOM and Liquid Crystal Institute, Kent State University, Kent, OH, 44242, USA

Version of record first published: 24 Sep 2006

To cite this article: Andy Ying-Guey Fuh, Tsung-Chin Ko, Ming-Shann Tsai, Chi-Yen Huang & Liang-Chy Chien (1998): Studies of Holographic Gratings Formed in Polymer-Dispersed Liquid Crystal Films and Their Dynamical Behavior, Molecular Crystals and Liquid Crystals Science and Technology. Section A. Molecular Crystals and Liquid Crystals, 321:1, 365-381

To link to this article: http://dx.doi.org/10.1080/10587259808025103

Mol. Cryst. Liq. Cryst., Vol. 321, pp. 365–381
Reprints available directly from the publisher
Photocopying permitted by license only

Published by license under
the Gordon and Breach Science
Publishers imprint.
Printed in Malaysia.

Studies of Holographic Gratings Formed in Polymer-Dispersed Liquid Crystal Films and Their Dynamical Behavior

ANDY YING-GUEY FUH, TSUNG-CHIN KO, MING-SHANN TSAI, CHI-YEN HUANG, and LIANG-CHY CHIEN[a]
Department of Physics, National Cheng-Kung University, Tainan, Taiwan 701, ROC; [a]Chemical physics, ALCOM and Liquid Crystal Institute, Kent State University, Kent, OH 44242, USA

We have developed an economic liquid crystal-polymer dispersion material that can be used for storing optical holographic images, The obtained results show that the written grating-holograms are permanent, but are electrically switchable. Further, we studied the dynamical behavior and the temperature-dependence of the formed gratings. The gratings morphologies were also investigated using scanning electron microscopy (SEM). The results showed the thermal grating was competing with the grating due to photopolymerization. The former dominated in the initial period, Later, it was offset or quenched by the photopolymerization effect which eventually dominated and determined the characteristics of the final gratings whose diffraction efficiencies were found to have a good correlation with their SEM images.

Keywords: holographic storage; liquid crystal polymer dispersions; dynamics

INTRODUCTION

There has been intense interest in materials capable of recording holographic planar or volume gratings. These include inorganic[1-2] and polymeric[3-4] photorefractive crystals, liquid crystals[3-9], bacteriorhodopsin[10], semiconductor[11] and glasses[12]. Diffraction efficiency and lifetime of the image, both during storage in the dark and, more critically, during multipleread operations, are the most important properties required for a recording material to be applicable in a practical optical storage device, although other properties, such as cost, structural flexibility and ease of processing, are also very important. There are some advantages and limitations associated with those storage materials mentioned above. Of the photorefractive materials, for example, polymeric materials are more economic, have better structural flexibility and are easier for processing in comparison with their inorganic cousins. However, their main disadvantage is that the lifetime of the image is currently limited to a matter of hours, because the charge do not remain trapped for long[4]. Although 'fixing' of the holographic image can be done with inorganic material, it usually requires the use of a high field and/or time-consuming large-temperature cycle. The liquid crystalline systems that have been investigated in the context of persistent grating also involve large laser-induced temperature and phase changes due to the highly absorbing dye used in these studies[5-9].

Recently, the use of polymer-dispersed liquid crystal (PDLC) films to record optical interference patterns, e.g. holograms and gratings has been reported[13-14]. The formed grating/hologram is permanent, but can be electrically switchable. In this paper, we report the results obtained from the dynamical studies of gratings formed in PDLC films. Qualitative studies on phase separation in the PDLC films having various liquid crystal-polymer mixing ratios were first made using a light scattering method. We then investigated the dynamical behavior of gratings at various ambient temperatures. The gratings' morphologies were finally investigated using scanning electron microscopy (SEM) and were found to have a good correlation with the gratings' final diffraction efficiencies.

EXPERIMENTS

Figure l(a) shows the experimental setup for studying the dynamics of the gratings formed on the PDLC films. Two writing beams, $\boldsymbol{E_1}$ and $\boldsymbol{E_2}$ derived from an Ar$^+$ laser ($\lambda = 514.5$nm), intersected at an angle $\theta \sim 2.4^\circ$. They were unfocused, and had a beam diameter ~ 4mm.

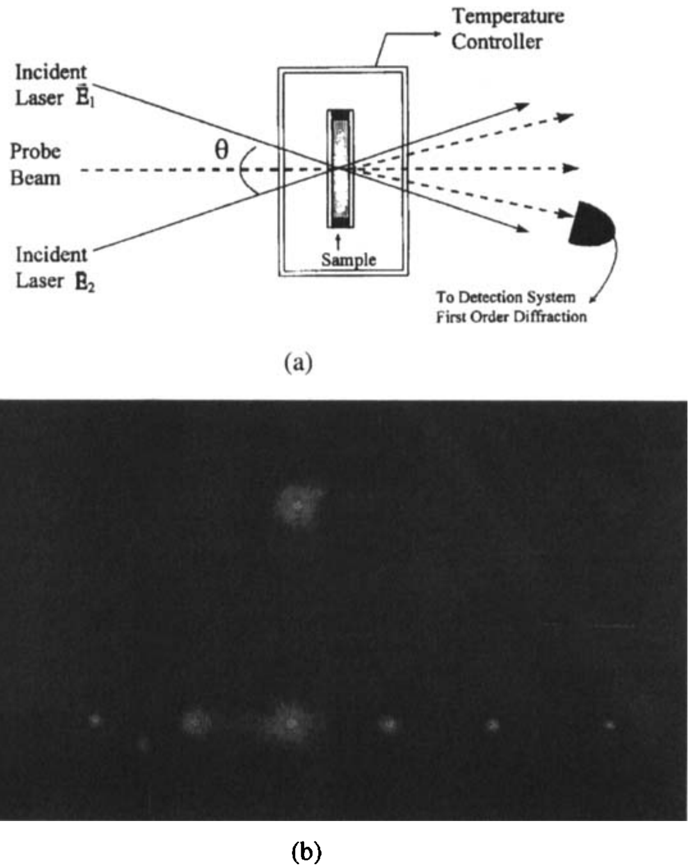

FIGURE 1 a) The experimental setup for studying the dynamical behavior of a PDLC grating at various temperatures; b) probed by an He-Ne laser, the final grating of a) yields the diffracted image (bottom) at the field-off condition, diffraction is switched off (upper image) with the application of an AC voltage ~140V onto the sample.

They each had approximately equal power ~75mW. Since they were coherent, an intensity interference pattern was set up in the intersecting region where the sample was placed. An unpolarized He-Ne laser was introduced in the plane determined by the E_1 and E_2 beams to probe the writing region of the sample. The intensity of one of the first-order diffracted beams was monitored as the grating was being formed.

The liquid crystal and polymer materials employed in this experiment were E7 and NOA65[15], respectively. A small amount of photoinitiator dye, Rose Bengal (RB), was added to the E7-NOA65 mixture. The function of this dye, with the presence of a coinitiator in the polymer, is to form free radicals, and then to initiate polymerization of NOA65 with the exposure of the film to a green-blue light. Drops of the homogeneously mixed E7-NOA65-dye mixture were then sandwiched between two indium-tin-oxide (ITO) coated glass slides separated by 36 μm thick plastic spacers to form a sample. During the experiments, the sample was placed in a temperature controller. The dynamical changes of the first order diffraction efficiency, for gratings formed in the PDLC films having ~ 20wt% E7, were studied as a function of time with the addition of various RB dye concentrations. The same dynamical experiments were then carried out for films having LC contents ~20wt% and 40wt% at various ambient temperatures with the addition of an optimum dye concentration of ~ 1.5wt%.

How the structure of an E7-NOA65-dye system develops during the curing process is also important. It helps in understanding the dynamical behavior of the formation of the gratings. A light scattering method was used to determine the onset of phase separation in this PDLC system. The sample was placed in a temperature chamber. Both an Ar^+ laser and a He-Ne laser were beamed on the sample simultaneously. These two beams made an angle ~ 1.2^0 and overlapped at the sample. The He-Ne laser was used to probe the transparency of the sample when it was cured by the Ar^+ laser. The onset of turbidity can be used to set an upper limit for the liquid crystal solubility in the polymer[16]. This has been applied to the determination of solubility limits in the PDLC films with apparently good results[17-18]. In other words, the transmission of the probe beam will be unchanged if no phase separation or no macroscopic phase separation occurs during curing. It should be noted that this method does not apply if the phase separation produces nematic domains much smaller than the wavelength of light. Qualitative, we therefore assume that no phase separation occurs if the transmission of the probe beam is unchanged in this case.

The morphologies of the cured gratings and the PDLC films were also examined using scanning electron microscopy (SEM). The preparation of SEM samples was reported in Ref. [14].

RESULTS AND DISCUSSIONS

Figure 1(b) shows the diffraction image (bottom) of a final grating yielded from Fig. 1(a), probed by a He-Ne laser in the field-off condition. The formed grating is permanent, but is electrically switchable. The diffracted beams can be switched off with the application of an AC voltage having $V_{rms} \cong 140V$. The result is shown in the upper image of Fig. 1(b).

Figure 2 shows the results obtained from the light scattering experiment with the films of E7-NOA65-dye system having various LC contents at room temperature. For samples having LC contents less than ~30wt%, no phase separation was observed. It occurred roughly at ~32wt%. Lovinger et al.[19] reported a detailed phase diagram of the E7-NOA65 (without dye). At room temperature, their result shows that phase separation occurs when the LC content is greater than 30wt%. It indicates that the addition of the photoinitiator dye does not significantly affect the phase separation.

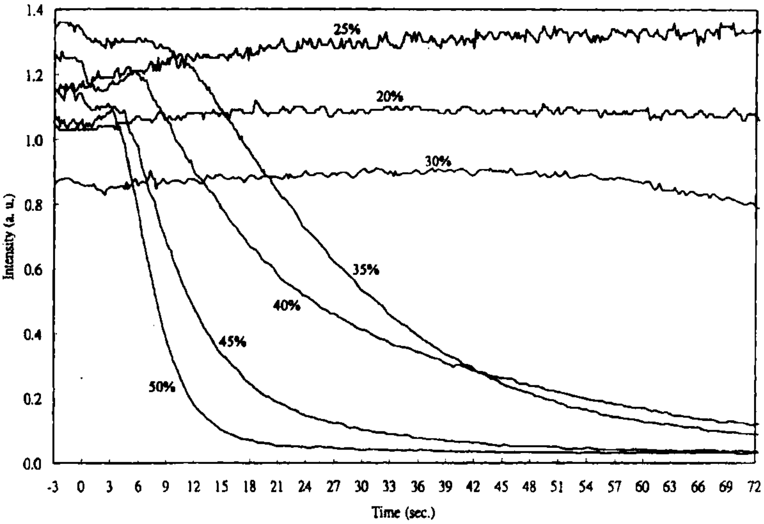

FIGURE 2 Results obtained from the light scattering experiment with the E7-NOA65-RB dye system. The dye concentration in the mixture was ~1.5wt%.

The light scattering experiment for a sample having 20wt% E7 as a function of time at temperatures above room temperature was also conducted. The result (not shown) shows that no phase separation occurs at these temperatures either. It is reasonable since the solubility increases as the ambient temperature increases.

Figure 3 shows the measured curves of the dynamical changes of the first-order diffraction efficiency (which is defined as the intensity of the diffracted beam divided by that of the probing beam) for a sample having ~20wt% E7, as a function of time, with the addition of various RB dye concentrations at room temperature. The probing laser was diffracted almost immediately after the Ar^+ laser beams were on at t=0 from the films with the addition of the RB dye. Without it, no grating effect was observed. The diffracted intensity was initially increased and peaked at ~ 8 seconds, then decreased, and finally increased again, and eventually become saturated. The peak is seen to be increasing with the dye concentration. This is assumed to be due to the laser-induced thermal grating caused by photo absorption of the dye. In a separate experiment, we measured the refractive index of the pre-polymer NOA65 as a function of the temperature. The result (not shown) showed the refractive index decreased linearly with an increase in temperature. The intensity interference pattern produced by the two Ar^+ laser beams sets up a thermal grating due to photoabsorption of the dye molecules. Mathematically, it can be written as

$$n=n_0+n_2I, \qquad (1)$$

where n_0 is the linear (under zero optical field) refractive index, n_2 is the Kerr coefficient which is negative in the present case, and I is the light irradiance.

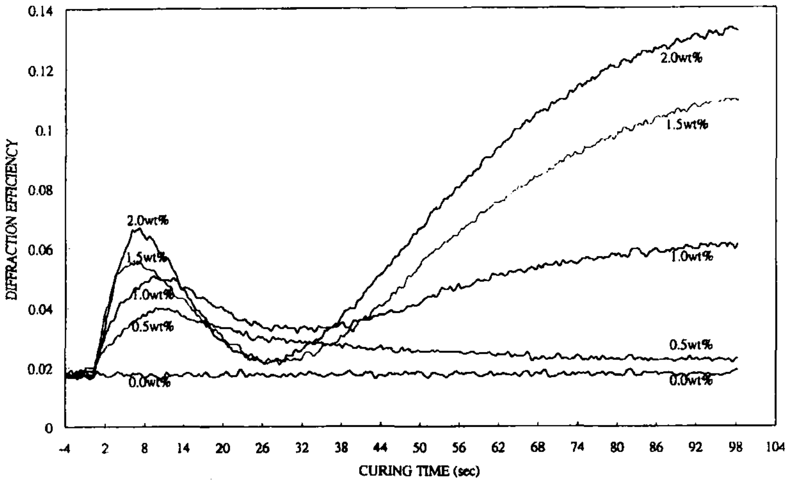

FIGURE 3 Dynamical changes of the first-order diffraction efficiency for gratings formed in PDLC film having ~20wt% E7 as a function of time with various RB dye concentrations.

The other contribution to the grating is from the photo-polymerization effect. These results can be understood by considering the chemical potential[20-21]. Photopolymerization preferentially initiates in the higher-intensity regions. This gives rise to a spatial pattern of monomer concentrations across the film. The consumption of monomers in these regions lowers their chemical potential. This gives rise to the diffusion of monomers towards the higher-intensity regions from the lower-intensity ones. On the other hand, as liquid crystal molecules are not consumed, their chemical potential increased in the higher-intensity regions over that in the lower-intensity regions due to the consumption of the NOA65 monomers. Hence there was a diffusion of LC molecules from the higher-intensity regions towards the lower-intensity ones, to equalize the chemical potential across the writing area. The molecular weight of the polymers in the higher-intensity regions increased from crosslinking to a much grater extent than the molecular weight of the polymers in the lower-intensity regions. Therefore, the intensity interference pattern produces a refractive index grating that is associated with the spatially varying molecular weight of the polymer molecules. This photopolymerization grating grew at a slower rate than the thermal grating, and was 180° out of phase with it. As a result, the diffracted intensity increased initially because of the rapid formation of the thermal grating as shown in Fig. 3. The intensity then decreased as the photopolymerization grating began to grow. When the gratings were equal in amplitude and opposite in phase, the diffracted intensity became zero. Finally the diffracted intensity increased again and eventually became saturated when the photopolymerization process was complete.

Figure 4 shows the results of the measured diffraction efficiencies of the sample having a LC content ~ 20wt% as a function of the curing time at various curing temperatures with the addition of ~ 1.5wt% RB dye.

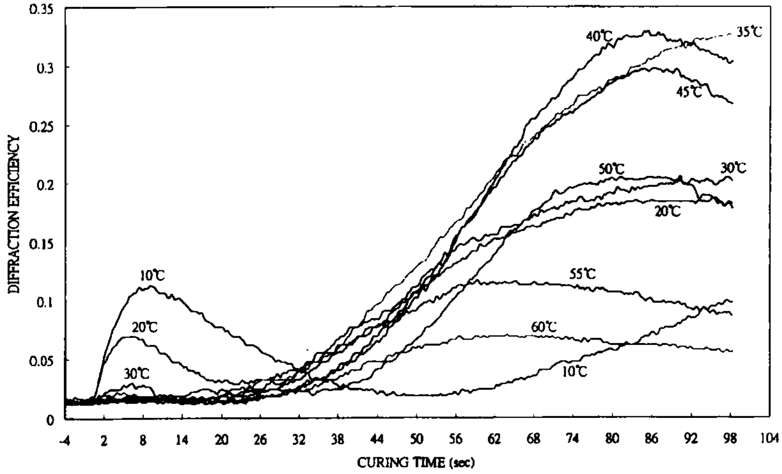

FIGURE 4 Dynamical changes of the first-order diffraction efficiency for PDLC gratings having ~20wt% E7 as a function of time at various curing temperatures.

The higher the curing temperature, the smaller the peak appearing initially. The thermal grating phenomenon can be observed till the temperature reaches ~ 35°C. It is believed that it is rapidly quenched by the higher diffusion speed of both the LC and the monomer molecules at higher curing temperatures with a lower viscosity as explained in Fig. 3. It is also seen that the diffraction efficiency of the final grating increases initially and then decreases. In order to explain this result, we investigated the SEM structures of these gratings, The results are shown in Fig. 5 (top-view). It is clear that there no LC droplets or domains in these images, and the results are consistent with those shown in Fig. 2. It is also note from Fig. 5 that the grating formed at 40°C has the sharpest stripes. Its final diffraction efficiency is therefore the highest as shown in Fig. 4.

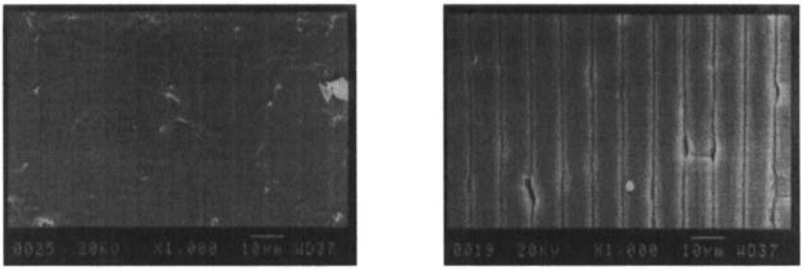

(a) 10℃ (d) 40℃

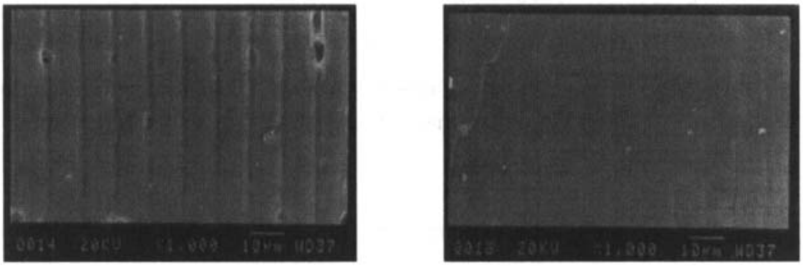

(b) 20℃ (e) 45℃

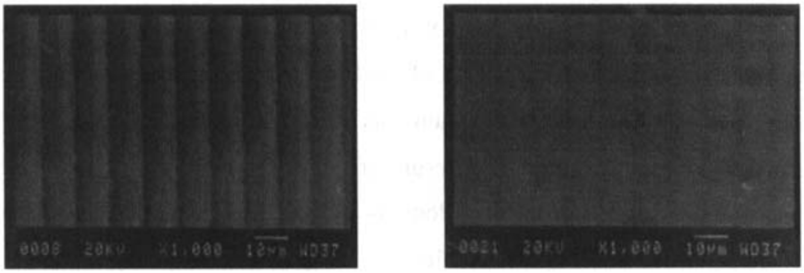

(c) 30℃ (f) 55℃

FIGURE 5 "Top-view" SEM morphologies of gratings formed in PDLC film having a LC content ~20wt% at various temperatures, (a) 10°C, (b) 20 °C, (c) 30 °C, (d) 40 °C, (e) 45 °C, (f) 55 °C.

Figure 6 shows the result obtained from the light scattering experiment for a sample having ~ 40wt% E7 as a function of time at various curing temperatures. The RB dye concentration added was ~ 1.5wt%. It is seen that the onset of turbidity occurs later for the samples cured at higher temperatures. This indicates that the solubility of LC in the polymer increases with increasing temperatures. For curing temperatures below 40°C, phase separation was observed. Above it, no macroscopic phase separation occurred. Figure 7 shows the top-view SEM morphologies of the same cells that gave the results shown in Fig. 6. The droplet morphologies were observed in samples cured at temperatures below 40°C. This is consistent with the result shown in Fig. 6. It is also noted from Fig. 7 that both the LC droplets size and the density are affected by the curing temperature. As the temperature increases, both the solubility of the LCs in the polymer and molecular diffusion rate increase.

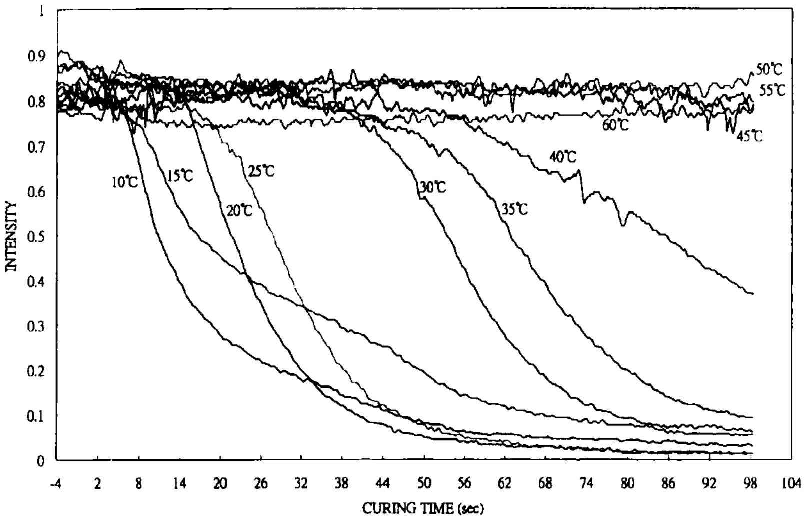

FIGURE 6 Results obtained from the light scattering experiment for the film having LC content ~40wt% at various curing temperatures. The RB dye concentration is ~1.5wt%.

The latter, in turn, increases the polymerization rate. As a result, the LC droplets for the sample cured at 10°C are small in size but dense. At 20°C, the droplets size is larger because of a higher diffusion rate of LC molecules; but the density is lower because fewer LC molecules separate from the polymer. At temperatures above 20°C, the amount of the LCs separating from the polymer is even less, so the droplets size gets smaller. As seen in Fig. 6 no macroscopic phase separation occurs at temperatures above 45°C. The SEM morphologies (Fig. 7) of the corresponding samples support this result.

Figure 8 shows the measured curves of the dynamical changes of the first-order diffraction efficiency for a sample having ~40wt% E7 as a function of time at various curing temperatures. It is seen that the peak appearing initially in Fig. 4 is not evident for these films. Since the LC content in these film is 40wt%, the mixture, has a lower viscosity than those having a LC content of 20wt%. As a result, the thermal grating effect is rapidly quenched by the diffusions of both the LC and the monomer molecules from the consideration of chemical potential. For the gratings written at temperatures below 40°C which show a phase separation as illustrated in Fig. 6, the formation of liquid crystal droplets begins at this time. It causes a rapid increase of diffraction efficiency starting at ~ t = 3s. When the droplets grow to have diameters comparable to the probing light wavelength, they scatter light effectively. The diffraction efficiency then decreases. For gratings written at temperatures above 45°C which show no phase separation, the final diffraction efficiencies do not change significantly as no droplets are formed.

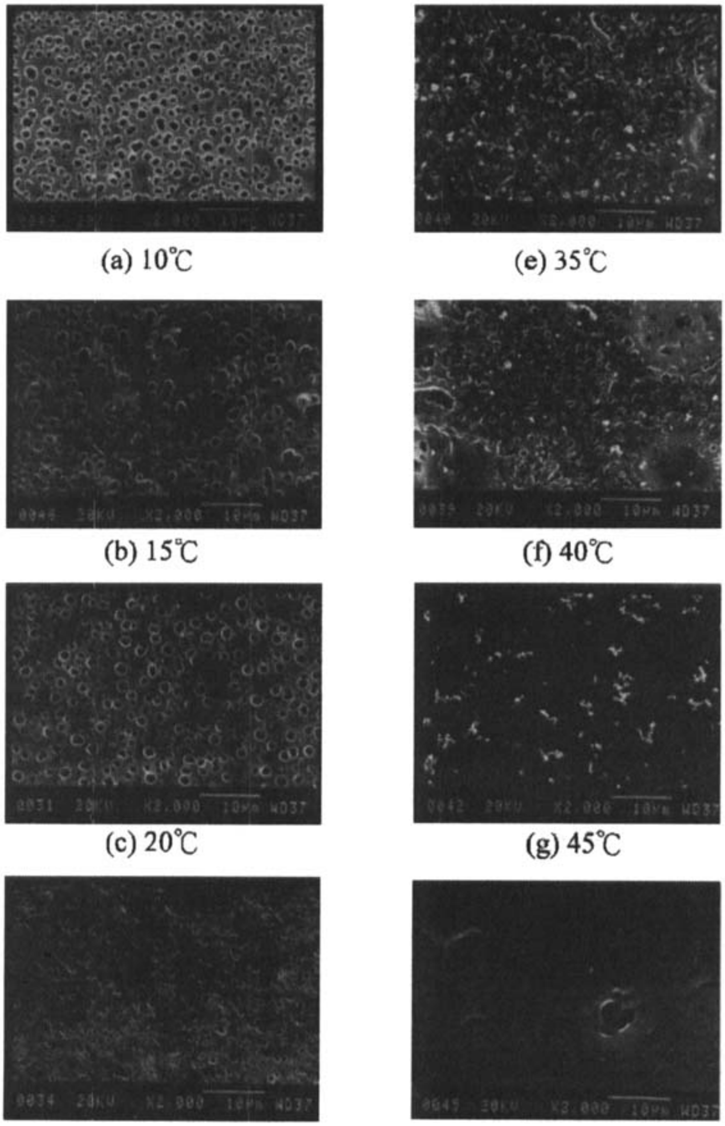

(a) 10℃ (e) 35℃

(b) 15℃ (f) 40℃

(c) 20℃ (g) 45℃

(d) 25℃ (h) 50℃

FIGURE 7 'Top-view' SEM images obtained from the light scattering experiment for the film having a LC content ~40wt% at various temperatures, (a) 10°C, (b) 15°C, (c) 20°C, (d) 25°C, (e) 35°C, (f) 40°C, (g) 45°, (h) 50 °C.

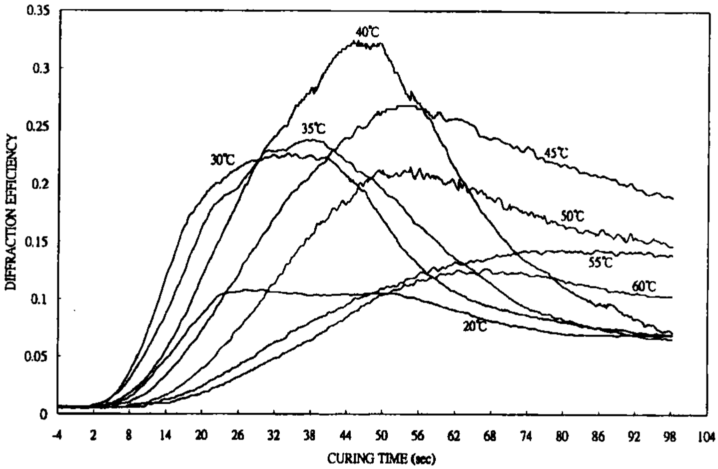

FIGURE 8 Dynamical changes of the first-order diffraction efficiency for PDLC gratings having ~40wt% E7 as a function of time at various curing temperatures. The dye concentration added in these samples was ~1.5wt%.

It is also seen from Fig. 8 that the diffraction peak (for gratings written at temperatures below 40^{o}C) and the saturated efficiency (for gratings written at temperatures above 45^{o}C) are affected by temperature change significantly. To study this effect, we also investigated the SEM morphologies of these gratings. The results are shown in Fig. 9 (top-view). It is clearly to see that there are droplets structures in the gratings written at temperatures below 40^{o}C. Above 45^{o}C, there exists no phase separation and, therefore, no droplet morphologies are observed in these samples. Furthermore, the LC and the polymer separate better when the temperature increases from 20 to 40^{o}C. This explains why the peak is higher for the grating written at a high temperature shown in Fig. 8. Another feature shown in Fig. 8 is that the final diffraction efficiency of the gratings formed above 45^{o}C decreases with increasing temperature. This can be understood from their SEM images shown in Fig.9.

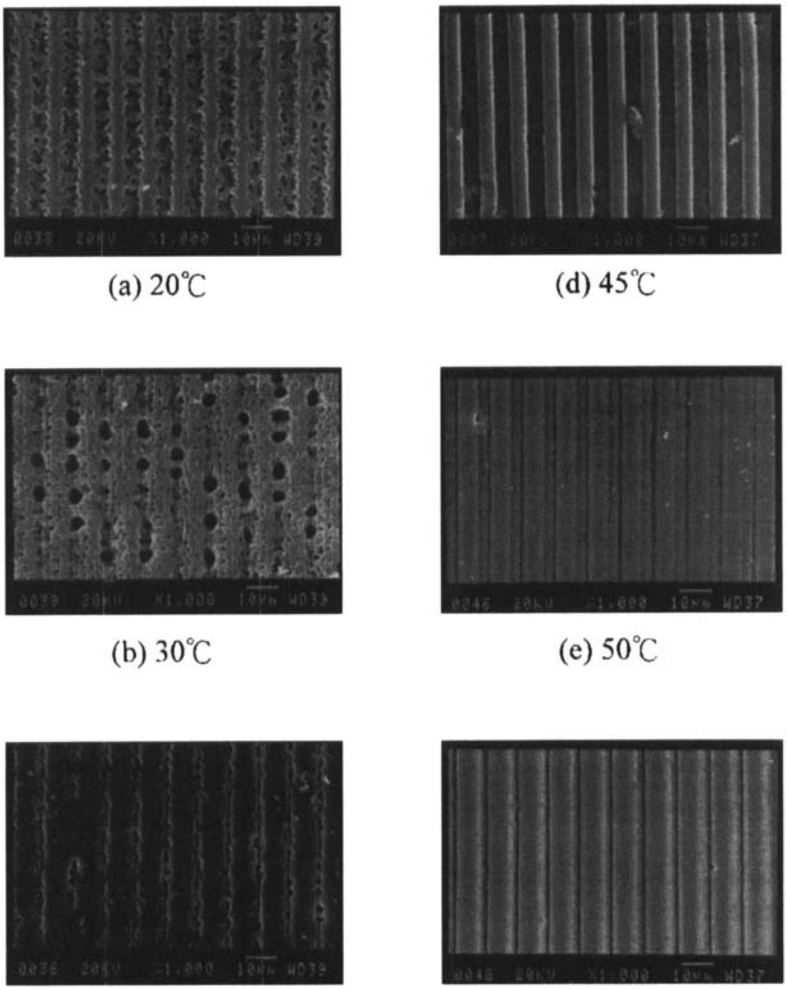
(a) 20℃

(d) 45℃

(b) 30℃

(e) 50℃

(c) 40℃

(f) 60℃

FIGURE 9 'Top-view' SEM morphologies of gratings formed in PDLC films having a LC content ~40wt% at various curing Temperatures, (a) 20°C, (b) 30°C, (c) 40°C, (d) 45°C, (e) 50°C, (f) 60°C.

At higher temperatures, the monomers diffuse faster. Thus, the polymerization rate is greater, and the polymer-rich regions become wider. This makes the width of the LC-rich regions smaller (trough stripes which result from the washout of LC-rich regions by hexane in the preparation of SEM samples). Also, the solubility is increasing with temperature. As a result, the refractive index difference between the LC-rich regions and the polymer-rich regions decreases with an increase in temperature.

In conclusion, we have studied both the phase separation and the dynamical behavior of the gratings formed in E7-NOA65-Rose Bengal dispersion films at various temperature. In the present case, the dynamical change of the first-order diffraction efficiency can be suitably explained by competition between the thermal grating and the grating due to photopolymerization. For the films having a LC content ~20wt% which showed no phase separation, we found that the thermal effect dominated initially at the temperatures below 35°C. Above it, the grating effect was rapidly quenched by the fast diffusive motion of both the LC and the monomer molecular in the film. This also explains the disappearance of the thermal grating effect in gratings formed in films having a LC content ~40wt%. Furthermore, the diffraction efficiencies of the final gratings were analyzed and found to be consistent with their SEM morphologies.

Acknowledgments

This work is supported partially by the National Science Council (NSC) of the Republic of China under Grants No. NSC 86-2112-M006-007, and partially by the Ministry of Education of the Republic of China. L.-C. Chien is supported by ALCOM.

References

[1.] A. Kewitsch, M. Segev, A. Yariv and R. Neurgaonkar, *Opt. Lett.*, **18**, 1262 (1993)

[2.] P. Gunter and J. P. Huignard(eds), *Photoreactive Materials and Their Applications.* Vols I and II (Springer-Verlag, Berlin, 1989).

[3.] S. Ducharme, J. C. Scoott. R. J. Tweig and W. E. Moerner, *Phys. Rev. Lett.*, **66**, 1846 (1991).

[4.] K. Meerholz, B. L. Volodin, S. B. Kippelen and N. Peyghambarian, *Nature*, **371**, 497 (1994).

[5.] W. M. Gibbons, P. J. Shannon, S. T. Sun and B. J. Swetlin, *Nature*, **351**, 49 (1991).

[6.] K. Ichimura, Y. Suzuki, T. Seko, T. Kawanichi, T. Tamaki and K. Aoki, *Jpn. J. Appl. Phys.*, **28**, 289 (1989).

[7.] A. G. –S. Chen and D. J. Brady, *Opt. Lett.*, **17**, 1241 (1992).

[8.] M. Eruch and J. Wendorff, *J. Opt. Soc. Am.*, **B 7**, 1428 (1990).

[9.] I. C. Khoo, H. Li and Y. Liang, *Opt. Lett.*, **19**, 1723 (1994).

[10.] O. Werner, B. Fisher and A. Lewis, *Opt. Lett.*, **17**, 241 (1992).

[11.] R. A. Linke, T. Thio, J. D. Chadi and G. E. Devlin, *Appl. Phys. Lett.*, **65**, 16 (1994).

[12.] A. Partoui, T. Erdogan, V. Mizrahi, P. J. Lemaire, A. M. Glass and J. W. Hwmig, *Appl. Phys. Lett.*, **64**, 821 (1994).

[13.] R. L. Sutherland, V. P. Tondiglia, and L. V. Notarajjan, *Appl. Phys. Lett.*, **64**, 1074 (1994).

[14.] A. Y. –G. Fuh, M. –S. Tsai, C. –Y. Huang, T. –C. Ko and L. –C. Chien, *Opt. Quant. Elect.*, **28**, 1535 (1996).

[15.] The liquid crystal E7 was purchased from BDH (British Drug House). The pre-polymer NOA65 was purchased from Norland Products, Inc.,New Brunswick, N. J., USA.

[16.] Paul S. Drzaic, *Liquid Crystal Dispersions* (World Scientific, Singapore, 1995), p.71

[17.] W. Smith and N. A. Vaz, *Mol. Cryst. Liq, Cryst.*, Tec, **A 237**, 243 (1993).

[18.] K. Rout and S. C. Jain, *Jpn. J. Appl. Phys.*, **30**, 1412 (1991).

[19.] J. Lovinger, K. R. Amundson and D. D. Davis, *Chem. Mater.*, **6**, 1726 (1994).

[20.] J. Bunning, L. V. Natarajjan, V. Tondiglia, R. L. Sutherland and W. W. Adams, *Polymer*, **36**, 2699 (1995).

[21.] Sutherland, L. V. Natarajjan, V. P. Tondiglia, T. J. Bunning and W. W. Adams, *SPIE*, **2404**, 132 (1995).